

1 **Title:** Complex hybridization between deeply diverged fish species in a disturbed ecosystem

2

3 **Authors:**

4

5 Shreya M. Banerjee^{1,2,3*+}, Daniel L. Powell^{1,2*}, Benjamin M. Moran^{1,2}, Wilson F. Ramírez-
6 Duarte^{2,4}, Quinn K. Langdon^{1,2}, Theresa R. Gunn^{1,2}, Gaby Vazquez², Chelsea Rochman⁴, Molly
7 Schumer^{1,2,5+}

8

9 ¹Department of Biology, Stanford University

10 ²Centro de Investigaciones Científicas de las Huastecas “Aguazarca”, A.C.

11 ³Center for Population Biology, University of California, Davis

12 ⁴Department of Ecology and Evolutionary Biology, University of Toronto

13 ⁵Hanna H. Gray Fellow, Howard Hughes Medical Institutes

14

15 *co-first authorship

16 +Correspondence to: smbanerj@ucdavis.edu and schumer@stanford.edu

17

18 **Abstract**

19

20 Over the past two decades researchers have documented the extent of natural hybridization
21 between closely related species using genomic tools. Many species across the tree of life show
22 evidence of past hybridization with their evolutionary relatives. In some cases, this hybridization
23 is complex – involving gene flow between more than two species. While hybridization is
24 common over evolutionary timescales, some researchers have proposed that it may be even more
25 common in contemporary populations where anthropogenic disturbance has modified myriad
26 aspects of the environments in which organisms live and reproduce. Here, we develop a flexible
27 tool for local ancestry inference in hybrids derived from three source populations and describe a
28 complex, recent hybridization event between distantly related swordtail fish lineages
29 (*Xiphophorus*) and its potential links to anthropogenic disturbance.

30

31

32 **Impact Summary**

33

34 As sequencing tools have advanced, we have found that barriers between animal species are
35 more porous than once thought. Researchers have found evidence for hybridization between
36 species throughout many branches of the tree of life. In some cases, these hybridization events
37 can involve more than two species. Here, we develop a flexible and user-friendly tool that can be
38 used to identify three-way hybrids and report the discovery of hybrids with ancestry from three
39 swordtail (*Xiphophorus*) species from an anthropogenically impacted site on the Río Calnali in
40 Hidalgo, Mexico. Researchers have studied hybrids between two *Xiphophorus* species along this
41 river for decades, but this is the first documented case of hybridization involving three species.
42 We explore hypotheses for what drove this hybridization event, including anthropogenic
43 pollutants and reduced water quality.

44

45 Introduction

46

47 Hybridization, or genetic exchange between species, is common in diverse organisms
48 across the tree of life, and can have important evolutionary consequences (Moran *et al.*, 2021).
49 The genetic, ecological, and evolutionary outcomes of hybridization are varied, from facilitating
50 rapid adaptation to exposing genetic incompatibilities. Examples from the recent literature
51 include introgression as a source of genetic rescue (Oziolor *et al.*, 2019) and hybridization
52 resulting in decreased tolerance of thermal stressors (Payne *et al.*, 2022). While evidence of
53 ancient introgression in the genomes of diverse taxa suggests that hybridization is common in the
54 evolutionary history of many species (Moran *et al.*, 2021), a growing number of studies point
55 towards anthropogenic disturbance as contributing to the formation of new hybrid zones (Fisher
56 *et al.*, 2006; Kelly *et al.*, 2010; Pampoulie *et al.*, 2020). As humans modify habitats, there are
57 numerous mechanisms by which anthropogenic environmental disturbance can cause
58 hybridization. These include phenological changes (Chunco, 2014; Vallejo-Marín & Hiscock,
59 2016), species introductions (Oziolor *et al.*, 2019), habitat alterations that lead to new contact
60 zones (Kelly *et al.* 2010), and decreased encounter rates of conspecifics (Willis *et al.*, 2011).
61 Environmental disturbance, e.g., pollution with urban effluents and/or reduced water quality, can
62 also directly impact sensory communication, disrupting signals used in mate choice (Seehausen
63 *et al.*, 1997; Fisher *et al.*, 2006; Powell *et al.*, 2022).

64 Hybridization between pairs of species has been intensively studied for several decades,
65 but a growing body of literature highlights that hybridization events can be complex, involving
66 three or more species (Heliconius Genome Consortium 2012; Toews *et al.* 2018; Langdon *et al.*
67 2019; Grant and Grant 2020, Natola *et al.* 2022). These types of complex hybridization events
68 are likely to be more common in groups where many species are interfertile and have
69 overlapping ranges. The evolutionary consequences of these events are not as well understood.
70 One possible outcome is “conduit” introgression, where genetic exchange can occur between
71 species that are not in geographic contact through hybridization with a third species (Langdon *et al.*
72 2019; Grant and Grant 2020; Natola *et al.* 2022). Such dynamics could explain observations
73 in the empirical literature such as cases where gene flow is inferred between geographically
74 isolated species (Cui *et al.*, 2013); although there are other potential causes of these patterns
75 including introgression from a now extinct lineage (Ottenburghs, 2020).

76 *Xiphophorus* species and their hybrids from the Sierra Madre Oriental of eastern Mexico
77 have been intensively studied over two decades. Much of this work has focused on hybridization
78 between two sister-species from the “Northern swordtail” clade, *X. birchmanni* and *X. malinche*
79 (Fig. 1). Throughout its range *X. birchmanni* is sympatric with a distantly related species in the
80 “platyfish” clade, *X. variatus* (Fig. 1). *X. variatus* is also common at many sites where *X.*
81 *birchmanni* x *X. malinche* hybrids (i.e. Northern swordtail hybrids) are found, but does not reach
82 the high elevations inhabited by pure *X. malinche*. Genetic and historical estimates indicate that
83 hybridization has been occurring between *X. birchmanni* and *X. malinche* in the Río Calnali for
84 more than 40 generations (Rosenthal *et al.*, 2003; Schumer *et al.*, 2014, 2017). However, despite
85 extensive collections in regions where they co-occur over the last two decades, no hybrids
86 between *X. variatus* and *X. birchmanni* or *X. variatus* and *X. birchmanni* x *X. malinche* have
87 been reported.

88 Here, we characterize a newly discovered three-way hybridization event involving *X.*
89 *birchmanni* x *X. malinche* hybrids and *X. variatus* at an anthropogenically disturbed site on the
90 Río Calnali (hereafter the Tlalica site; Fig. 1). To facilitate this analysis, we develop an easy to

91 use and accurate extension of the *ancestryinfer* pipeline (Schumer *et al.*, 2020) that enables local
92 ancestry inference of individual hybrids formed from three source populations. We initially
93 identified three-way hybrids based on morphology, and confirmed our observations with whole
94 genome-sequencing and local ancestry inference. We also characterized water quality and
95 chemistry (relevant to the visual and olfactory environment) at Tlalica and other sites along the
96 Río Calnali to explore relationships between environmental disturbance and hybridization. Our
97 results hint at a connection between anthropogenic disturbance and hybridization in these deeply
98 diverged species with a long history of reproductive isolation in sympatry.
99
100

101 **Methods**

102

103 *Morphological evidence of hybridization between *X. variatus*, *X. birchmanni*, and *X. malinche**

104 Three-way hybrids were first identified at the Tlalica site based on their unusual
105 phenotype combinations. Male *X. variatus*, *X. birchmanni*, and *X. malinche* differ in several
106 traits (females are phenotypically similar in many *Xiphophorus* species). *X. malinche* has a
107 modification of the caudal fin known as the “sword” which is absent in the two other species and
108 *X. birchmanni* has a much larger dorsal fin compared to the other two species (Fig. 1). *X.*
109 *variatus* is characterized by a distinctive diamond body shape (Fig. 1A, 2A), and two horizontal
110 stripes composed of melanophores bracketing the lateral line. By comparison, *X. malinche*, *X.*
111 *birchmanni*, and their hybrids are more elongated (Fig. 2A) and have a single, broader horizontal
112 stripe. *X. variatus* have polymorphic melanophore tailspot patterns (described in Borowsky,
113 1980; Culumber & Rosenthal, 2013) that are distinct from the polymorphic melanophore patterns
114 present in some *X. birchmanni* and *X. birchmanni* x *X. malinche* hybrid individuals
115 (Rauchenberger *et al.*, 1990; Culumber, 2014; Powell *et al.*, 2020).

116 We noticed that two adult males sampled from Tlalica in June 2021 appeared to have *X.*
117 *variatus*-like characteristics, such as a diamond body shape and dual horizontal stripes, *X.*
118 *birchmanni*-like characteristics, such as large body size and large rounded dorsal fins, and *X.*
119 *malinche*-like characteristics, such as short sword extensions (Fig. 2). For these fish and
120 additional male three-way hybrids identified in subsequent collections (n = 12) we measured
121 standard length, body depth, peduncle depth, caudal fin length, dorsal fin width, dorsal fin
122 height, and sword length from photographs of anaesthetized adult male fish using ImageJ (Fig.
123 S1; Schneider, Rasband, & Eliceiri, 2012). We included phenotypes of *X. birchmanni* x *X.*
124 *malinche* hybrids from a nearby population (Calnali Low; n = 9) and of pure parental species
125 individuals from sites where hybrids have not previously been reported (*X. variatus* from
126 Coacuilco: n = 27, *X. birchmanni* from Coacuilco: n = 24; *X. malinche* from Capac: n = 5) (Fig.
127 1C). We performed principal component analyses to assess morphological differences between
128 groups.

129

130 *Genomic libraries of putative hybrids*

131 For the two male individuals collected in June of 2021 that were morphologically
132 identified as likely three-way hybrids, we produced high-coverage whole genome data (Table
133 S1) following Schumer *et al.* (2016, 2018). Briefly, we extracted DNA from fin clips using half
134 reactions of the Agencourt DNAdvance kit. DNA was sheared by sonication and end-repaired
135 with dNTPs, T4 DNA polymerase, Klenow DNA polymerase, and T4 polynucleotide kinase,
136 then A-tailed with Klenow exonuclease and dATP. Universal Illumina adapters were ligated onto
137 the A-tailed sample using DNA ligase. Samples were purified with the Qiagen PCR Purification
138 kit between steps. Samples were PCR amplified for 12 cycles using the Phusion PCR kit. After
139 amplification, the final PCR product was purified with 18% SPRI beads and sent to Admera
140 Health (South Plainfield, NJ, USA) for sequencing on an Illumina HiSeq 4000.

141

142 *Preliminary investigation of three-way hybrids with sppIDer*

143 We used the competitive mapping and read depth analysis pipeline, sppIDer (Langdon *et*
144 *al.*, 2018) as an initial approach to investigate the potential genetic contributions to the two male
145 fish sampled in June of 2021 from Tlalica. We created a combined fasta file by concatenating *X.*
146 *birchmanni*, *X. malinche*, and *X. variatus* reference genomes (described in Powell *et al.*, 2021).

147 Reads from the high coverage Tlalica males were mapped to this combination reference genome
148 and uniquely mapped reads were used by sppIDer to estimate the proportion of the genome
149 derived from each species (see Langdon *et al.*, 2018).

150

151 *PSMC and analysis of whole genome sequences*

152 Raw Illumina reads from an *X. variatus* individual from the Coacuilco population
153 (previously sequenced by Powell *et al.*, 2020) were aligned to a *de novo* assembly derived from
154 *X. variatus* that was scaffolded with cactus (Armstrong *et al.*, 2020) to a chromosome-level *X.*
155 *birchmanni* assembly (Powell *et al.*, 2020). Alignment of reads was performed using *bwa* (Li &
156 Durban, 2009). We used PicardTools and *GATK* (Van der Auwera & O'Connor, 2020) to realign
157 mapped reads around indels and call variant sites in a gvcf format. Individual jobs were run for
158 each chromosome for indel realignment and variant calling. We combined gvcf files for all
159 chromosomes using *bcftools* (Danecek *et al.*, 2021). We filtered variant and invariant sites from
160 this combined gvcf file as previously described (Schumer *et al.*, 2018). Briefly, we used hard-call
161 thresholds for variant quality scores recommended by *GATK* and previously validated in
162 swordtails using pedigree data (Schumer *et al.*, 2018). For both variant and invariant sites, we
163 masked sites within 5 bp of an INDEL or >2X or <0.5X the average genome-wide coverage. To
164 generate a pseudo-fasta file reflecting variant and masked sites, we used a custom script to
165 generate an insnp file (https://github.com/Schumerlab/Lab_shared_scripts). We used *seqtk*
166 (<https://github.com/lh3/seqtk>) to generate a new fasta file with variant sites and masked sites
167 updated to reflect the *X. variatus* individual being analyzed.

168 We next used this data to infer changes in historically effective population size through
169 time using the Pairwise Sequential Markovian Coalescence approach (PSMC, Li & Durbin,
170 2011). We used a custom script to convert the fasta file to a fastq file (the required input format
171 for PSMC) with uniform quality scores, (https://github.com/Schumerlab/Lab_shared_scripts) and
172 used *seqtk* to exclude scaffolds that did not belong to the 24 major *Xiphophorus* chromosomes.
173 We assumed a mutation rate of 3.5×10^{-9} per basepair per generation, a generation time of half a
174 year, and set the -r parameter to 2 (Schumer *et al.*, 2018). We compared these results for *X.*
175 *variatus* to those previously published for *X. birchmanni* and *X. malinche* (Schumer *et al.*, 2018).
176 For comparison to our results for *X. variatus*, we included only one sample per species.

177

178 *Low-coverage whole genome sequencing of individuals collected from Tlalica and nearby sites*

179 We extracted DNA from fin clips using the Agencourt DNAdvance bead-based kit as
180 specified by the manufacturer except that we used half-reactions. We prepared tagmentation-
181 based libraries for low-coverage whole genome sequencing as previously described (Payne *et al.*
182 2022). Briefly, DNA was enzymatically sheared using the Illumina Tagment DNA TDE1
183 Enzyme and Buffer Kit, amplified in a dual-indexed PCR reaction for 12 cycles, pooled, and
184 bead purified with 18% SPRI magnetic beads. Libraries were sent to Admera Health (South
185 Plainfield, NJ, USA) to be sequenced on a HiSeq 4000.

186

187 *Design and performance tests of three-way local ancestry inference*

188 To perform three-way local ancestry inference, we adapted our previously developed
189 pipeline, *ancestryinfer* (which only allowed for two source populations; Schumer *et al.*, 2020), to
190 accommodate three reference genomes and source populations. Briefly, we modified the
191 program to detect whether two or three reference genomes were provided in the configuration
192 file (see Appendix 1 – user manual). When three reference genomes are provided, *ancestryinfer*

193 maps reads to all three genomes and identifies and excludes any reads that do not map uniquely
194 to any of the three references. Using the coordinate space of reference genome 1, it tabulates
195 counts for each allele at each ancestry-informative site and runs AncestryHMM in the three
196 source population mode (Corbett-Detig & Nielsen, 2017). Users can optionally provide priors for
197 the number of generations since initial admixture for each source population and priors for
198 admixture proportions from each source population.

199 We searched for candidate ancestry-informative sites from high coverage whole genome
200 sequences (*X. variatus* n=2, *X. malinche* n=4, *X. birchmanni* n=26; samples from Schumer *et al.*,
201 2018; Powell *et al.*, 2020, 2021). Although we use a small number of high coverage samples in
202 this initial step based on available data, we filter sites using a large number of individuals of each
203 species (see below). We identified biallelic sites that differentiated any of the three focal
204 species. Initial analysis suggested that issues with accuracy arise from imbalance in the number
205 of ancestry-informative sites between pairs of species. We thinned to an approximately
206 equivalent number of informative sites between all pairs of species. To do so, we retained all
207 ancestry-informative sites that distinguished *X. birchmanni* and *X. malinche*, and every other site
208 that distinguished *X. variatus* from either of these two species.

209 We refined this candidate set of ancestry-informative sites using low-coverage population
210 data from each species (*X. malinche* n=28, *X. birchmanni* n=107 – Schumer *et al.*, 2018; *X.*
211 *variatus* n=145 – this study). Note that per basepair heterozygosity is much lower in *X. malinche*,
212 approximately ¼ of the levels observed in *X. birchmanni* or *X. variatus* (0.0003 per basepair
213 versus ~0.001 respectively). Low nucleotide diversity in *X. malinche* is attributable to low
214 historical effective population sizes in this species (Schumer *et al.*, 2018). Average coverage per
215 individual was ~1X. Because this is low coverage data, we did not perform explicit variant
216 calling but instead used bcftools mpileup to determine the observed counts for each allele at each
217 candidate ancestry-informative site in the three source populations. We then excluded ancestry-
218 informative sites that did not have equal to or greater than a 90% frequency difference between
219 at least one pair of species (e.g. *X. birchmanni* vs *X. malinche*, *X. birchmanni* vs *X. variatus*, *X.*
220 *malinche* vs *X. variatus*). This resulted in a final set of 997,366 ancestry-informative markers
221 throughout the 750 Mb genome.

222 Using this set of ancestry-informative sites and estimated parental allele frequencies
223 determined from the individuals described above, we ran *ancestryinfer* on a set of parental
224 individuals that were not used in the training datasets ($n_{\text{variatus}} = 30$; $n_{\text{birchmanni}} = 12$; $n_{\text{malinche}} = 10$)
225 as a first performance check on empirical data. We found that *ancestryinfer* correctly inferred
226 that these individuals were unadmixed and derived from the correct parental population (Fig.
227 S2). We also performed a similar analysis on hybrids from *X. birchmanni* x *X. malinche* hybrid
228 populations that are allopatric with respect to *X. variatus* (Tonicapá, n=30, and Tlatemaco, n=
229 23; Fig. S3). See Supporting information 1 for additional performance testing and simulations.

230 We note that we do not have access to any populations in which *X. birchmanni* does not
231 co-occur with *X. variatus*. Thus, if there was admixture between *X. birchmanni* and *X. variatus*
232 in the *X. birchmanni* source populations that we have failed to detect, our approach could
233 underestimate the degree of contemporary gene flow between these species.

234 235 *Local ancestry inference and data processing of three-way hybrids*

236 We proceeded with local ancestry analysis of individuals collected from the Tlalica
237 population (n=64) and previously collected samples from upstream (n=553; Table S2) and
238 downstream (n=25) of this site on the Río Calnali. We also ran *ancestryinfer* on all sequenced

239 pure *X. birchmanni* and *X. variatus* from Coacuilco, an allopatric site in a different drainage, to
240 confirm their ancestry (n=745; samples from Powell *et al.*, 2020 and this study; Table S3). For
241 hybrid individuals from the Río Calnali, we provided priors for admixture proportions from the
242 three source populations based on sppIDer results. *ancestryinfer* accepts priors for the time since
243 initial admixture for all source populations (see Corbett-Detig & Nielsen, 2017). Based on past
244 results for *X. birchmanni* x *X. malinche* (Schumer *et al.* 2014, 2017) and the results of an initial
245 run of *ancestryinfer* without specifying a prior for admixture time, we set the prior admixture
246 time between *X. malinche* and *X. birchmanni* to 50 and the prior admixture time between this
247 admixed population and *X. variatus* to 2. We excluded individuals with fewer than 500,000
248 reads, based on previous simulation results that indicated accuracy of local ancestry inference is
249 reduced in individuals with <0.2X coverage (Schumer *et al.*, 2020). This analysis resulted in
250 posterior probabilities for each of the six possible ancestry states (homozygous *X. birchmanni*,
251 homozygous *X. malinche*, homozygous *X. variatus* and each possible heterozygous combination)
252 at 900,343 ancestry-informative sites throughout the genome.

253 We used a posterior probability threshold of 0.9 to convert ancestry probabilities to hard-
254 calls. For ancestry-informative sites that did not have a probability of ≥ 0.9 for any ancestry state,
255 we converted the probabilities for those sites to NA. The average level of missing data in three-
256 way hybrid individuals after imposing this hard-call threshold was 0.03%.

257

258 *Water quality and chemistry at Tlalica*

259 Tlalica is ~1 km away from the municipal landfill of the city of Calnali and 2.7 km
260 downstream from the outfall of a sewage treatment plant. During the wet season, we observed a
261 small tributary running through the municipal landfill into the Río Calnali approximately 250
262 meters upstream of Tlalica. On one sampling occasion, we observed sewage effluent flowing
263 into the river from the treatment plant upstream of Tlalica. On another occasion a break in the
264 sewer line upstream of the treatment plant led to contamination of the river ~3 km upstream of
265 the sampling site. Accordingly, we expected water quality at the Tlalica site to be lower than
266 upstream sites (Fig. 1), and hypothesize that this could contribute to the hybridization observed
267 between distantly related *Xiphophorus* species.

268 We collected water samples in May and June of 2022 at a relatively undisturbed upstream
269 site (Plank), and at the three sites where we found genetic evidence of one or more three-way
270 hybrids (see Results; Plaza, Calnali Low, and Tlalica; Fig. 1). All focal sites contained both *X.*
271 *variatus* and *X. birchmanni* x *X. malinche* hybrids. We measured fluorescent dissolved organic
272 matter (DOM) and turbidity using an EXO2 multiparameter sonde (YSI, Yellow Springs, OH).
273 We used a 9300 colorimeter (YSI, Yellow Springs, OH) to quantify ammonia. We quantified
274 concentrations of dissolved copper (using a 0.45 μm polyethersulfone membrane, and
275 acidification to pH ~2.0 with trace metal grade nitric acid) in water using inductively coupled
276 plasma mass spectrometry (ICP-MS) by following the modified version of the
277 APHA3030B/6020A methods. See Supporting information 2 for additional water quality and
278 chemistry metrics collected.

279

280

281

282 Results

283

284 *Morphological results and demographic survey of the Tlalica population*

285 Three-way hybrids were morphologically distinct from pure parental individuals and
286 from *X. birchmanni* x *X. malinche* hybrids found in nearby populations (Fig. 2, Table S4). They
287 were most morphologically distinct from other groups analyzed along PC1 (74.9% of variation
288 explained), and clustered with *X. malinche*, *X. variatus*, and Northern swordtail hybrid
289 individuals along PC2 (21.6% of variation explained; Fig. 2).

290 Based on visual phenotypes, a large majority of individuals collected from the Tlalica site
291 in May 2021, November 2021, February 2022, and May 2022 were classified as *X. variatus*.
292 From visual phenotypic data alone, *X. variatus*-like individuals outnumbered *X. birchmanni* x *X.*
293 *malinche* hybrids by ~33:1 (based on 571 individuals collected in May 2022). Genotype data
294 from a subset of fish collected at Tlalica that were categorized as *X. variatus* indicate that we can
295 accurately differentiate them based on morphology alone (Fig. S4).

296

297 *History of divergence between X. variatus, X. birchmanni, and X. malinche*

298 *X. variatus* and the Northern swordtail clade to which *X. birchmanni* and *X. malinche*
299 belong are deeply divergent (Fig. 1; Schumer *et al.* 2014; 2016; 2018). Pairwise sequence
300 divergence between *X. birchmanni* – *X. variatus* and *X. malinche* – *X. variatus* is 1.42% and
301 1.43% respectively. Because *X. malinche* has undergone a severe recent bottleneck (see below,
302 Fig. 1), we focus on comparisons between *X. birchmanni* and *X. variatus* here. The per-site
303 heterozygosity (θ_π) for *X. variatus* is 0.11%, similar to that observed in *X. birchmanni* (0.12%;
304 Schumer *et al.*, 2018). Assuming that the ancestral θ is close to that of *X. birchmanni* and *X.*
305 *variatus*, we estimate the divergence time between the two clades is approximately 7.5 in units of
306 $4N_e$ generations (using the relationship $T_{div/2N_e} = D_{xy}/\theta - 1$).

307 Comparing PSMC results for *X. variatus* to those previously inferred for *X. birchmanni*
308 and *X. malinche* highlights differences in the inferred effective population sizes of each species
309 over time (Fig. 1). We estimated the long-term effective population size of *X. variatus* from one
310 individual to be approximately 50,000 individuals, similar to our previous estimates for *X.*
311 *birchmanni* (48,000–53,000; Powell *et al.*, 2021). However, the timing and extent of
312 demographic fluctuations varies between the two species (Fig. 1). *X. malinche* differs more
313 substantially in its inferred demographic history from both *X. birchmanni* and *X. variatus* given
314 the strong bottleneck that has persisted through much of its recent history (Fig. 1; Schumer *et al.*,
315 2018).

316 Assuming a long-term effective population size of 50,000 individuals, and the divergence
317 time in $4N_e$ generations calculated above, we estimate the divergence time between *X. variatus*
318 and *X. birchmanni* (and *X. malinche*) to be approximately 1.5 million generations.

319

320 *Ancestry analysis of Tlalica hybrids and nearby populations*

321 Initial analysis of genomic data with sppIDer indicated that males visually categorized as
322 three-way hybrids were likely hybrids between *X. variatus*, *X. birchmanni*, and *X. malinche* (Fig.
323 S5). We found that for each Tlalica male 52% of the reads preferentially mapped to the *X.*
324 *variatus* reference genome, 30-34% mapped to the *X. birchmanni* reference genome, 26-29%
325 mapped to the *X. malinche* reference genome.

326 This finding led us to develop local ancestry inference for three-way admixture for these
327 species (see Methods). The results of our local ancestry inference analysis indicated that

328 seventeen individuals sequenced from the Tlalica population were early generation hybrids
329 between *X. variatus*, *X. birchmanni*, and *X. malinche*. Among individuals at Tlalica with
330 Northern swordtail ancestry, we estimate the frequency of three-way hybrids to be ~10% of
331 individuals; this estimate is based on individuals collected before May 2022 since in later
332 samples we selectively collected suspected three-way hybrids (Fig. 3B; Table S5). Three-way
333 hybrid individuals derived ~50-75% of their genomes from *X. variatus*.

334 Samples collected from Tlalica that did not show evidence of ancestry derived from all
335 three species fell into two categories: hybrids between *X. birchmanni* and *X. malinche* and pure
336 *X. variatus* (Fig. 3). Hybrids between *X. birchmanni* and *X. malinche* derived approximately 25-
337 75% of their genomes from either of these parent species (Fig. 3). This is consistent with
338 admixture proportions observed in hybrids between *X. birchmanni* and *X. malinche* at sites up
339 and downstream of Tlalica (Fig. 1; Fig. 2; Schumer *et al.*, 2017). This suggests that three-way
340 hybrids with *X. variatus* originated from admixture with already extant *X. birchmanni* x *X.*
341 *malinche* hybrids. Indeed, *X. birchmanni* and *X. malinche* ancestry tract lengths in three-way
342 hybrids are similar to those observed in *X. birchmanni* x *X. malinche* hybrids at nearby sites
343 (average minor parent ancestry tract length ~150-200 kb; Schumer *et al.*, 2017). Samples
344 preliminarily categorized as *X. variatus* based on morphology from the Tlalica population show
345 no evidence of introgression from *X. birchmanni* or *X. malinche* (Fig. S4).

346 Given the proximity of Tlalica to previously sampled sites on the Río Calnali (~3 km),
347 and the fact that *X. variatus* is sympatric with several *X. birchmanni* x *X. malinche* hybrid
348 populations along the river (Fig. 1, Fig. 3), we asked if there is evidence of three-way
349 hybridization at other sites. We performed three-way local ancestry inference on 578 historically
350 and newly collected samples from other sites on the Río Calnali from 2003 to 2022 (previously
351 assumed based on morphology to represent *X. birchmanni* x *X. malinche* hybrids; Schumer *et al.*,
352 2017; Table S2). We identified only two three-way hybrids from these sites — a female from the
353 Plaza site who derived ~25% of her genome from *X. variatus* and a male from Calnali Low who
354 derived 50% of his genome from *X. variatus* (Fig. 3; 0.4% of sequenced specimens from other
355 sites).

356
357 *Inference about the generation of admixture using ancestry tract lengths*

358 Observed admixture proportions for three-way hybrids (25-75% *X. variatus* ancestry
359 across all samples) suggests that these individuals might be early generation hybrids between *X.*
360 *variatus* and Northern swordtail hybrids. Some of these samples are clearly first generation
361 hybrids between *X. variatus* and *X. birchmanni* x *X. malinche* hybrids based on local ancestry
362 patterns (N=17; Fig. 3). These individuals derived 50% of their genomes from *X. variatus* and
363 were heterozygous for *X. variatus* ancestry at nearly every ancestry-informative site across the
364 genome (>99.5% across individuals; Fig. 3). The few sites inferred to be homozygous *X.*
365 *variatus* are consistent with our expected error rate (see Methods).

366 Two individuals with substantial *X. variatus* ancestry did not have ancestry patterns
367 consistent with those expected for first generation hybrids. Both their observed admixture
368 proportions (25% and 75% *X. variatus*, respectively) and the lengths of ancestry tracts
369 heterozygous or homozygous for *X. variatus* ancestry indicate that these individuals are likely
370 backcrosses between a three-way hybrid with a pure *X. variatus* individual (Fig. 3). The
371 identification of two second-generation three-way hybrids indicates that hybrids between *X.*
372 *birchmanni*, *X. malinche*, and *X. variatus* are at least partially fertile.

373 Since the mitochondrial genome is maternally inherited, it allows us to infer the likely
374 maternal ancestry for the three-way hybrids identified. All three-way hybrids (n = 19) sequenced
375 had mitochondrial ancestry derived from either *X. birchmanni* or *X. malinche* (Table S5),
376 suggesting that the mothers of all three-way hybrid individuals sampled to date were *X.*
377 *birchmanni* x *X. malinche* hybrids. Skews in maternal ancestry may be the result of population
378 demography, differences in the strength of mate discrimination across groups, or impacts of
379 cross direction on the viability of hybrids.

380

381 *Water quality and chemistry analysis*

382 Dissolved organic matter, ammonia, dissolved copper, and turbidity were all elevated at
383 the Tlalica sampling site in comparison with the relatively undisturbed upstream Plank site when
384 we collected water samples in the spring of 2022 (Fig. 2B). Two sites between Plank and Tlalica
385 where three-way hybrids were detected at low frequencies, Plaza and Calnali Low, had
386 intermediate values of dissolved organic matter, ammonia, and dissolved copper (Fig. 2B). With
387 one season of data collection, we focus on qualitative patterns in the results. However, our results
388 show a pattern of elevated pollution and turbidity at sites with higher frequencies of
389 hybridization between *X. variatus* and *X. birchmanni* x *X. malinche* hybrids. Additional water
390 quality and chemistry metrics are shown in Fig. S6.

391 Discussion

392

393 Here we characterize wild caught *Xiphophorus* individuals with ancestry from three
394 parental species — *X. variatus*, *X. birchmanni*, and *X. malinche* — using multiple approaches.
395 Though *X. birchmanni* x *X. malinche* hybrids were first reported nearly two decades ago
396 (Rosenthal *et al.* 2003), hybridization with *X. variatus* has not been previously reported. These
397 results are remarkable given that *X. variatus* have ~1.5% sequence divergence from the Northern
398 swordtail clade. This is similar to divergence between chimpanzees (*Pan troglodytes*) and
399 gorillas (*Gorilla spp.*) (Chen & Li, 2001), highlighting the unusually deep nature of this
400 hybridization event.

401 To facilitate this work, we developed a user-friendly pipeline for running local ancestry
402 inference in hybrids which derive their genomes from three source populations, as well as a
403 collection of simulation scripts to test expected performance (see Appendix 1). Although several
404 methods have been developed that accommodate local ancestry inference with three source
405 populations (reviewed in Wu *et al.* 2021), there are few pipelines available that allow researchers
406 to move from raw reads to probabilities of ancestry across the genome. By expanding our
407 previously developed local ancestry inference pipeline and simulation scripts (Schumer *et al.*,
408 2020), we are able to provide a toolkit that can be used by researchers to study complex
409 hybridization events in diverse species groups.

410 The existence of natural hybrids between *X. variatus* and *X. birchmanni* x *X. malinche*
411 hybrids is surprising. Despite extensive collections over the past two decades and substantial
412 range overlap between *X. variatus*, *X. birchmanni*, and *X. birchmanni* x *X. malinche* hybrids,
413 there are no reports of contemporary hybridization involving *X. variatus*. However, past work
414 has identified a small genomic contribution from the lineage leading to *X. variatus* to the
415 ancestors of *X. birchmanni* and *X. malinche* (Schumer *et al.* 2018), which indicates that gene
416 flow has occurred historically. This event contributed ~2-4% of the genome to present-day *X.*
417 *birchmanni* and *X. malinche* (Schumer *et al.* 2018). Together with our present data, this suggests
418 that hybridization between these groups is possible, albeit rare.

419 *X. variatus* are sympatric with natural *X. malinche* x *X. birchmanni* hybrid populations at
420 several upstream sites along the Río Calnali where we have found no evidence of three-way
421 hybridization. In our analyses of 642 Northern swordtail individuals from sites along the river,
422 we have identified fifteen individuals with three-way hybrid ancestry at Tlalica, one individual at
423 Plaza, and one individual at Calnali Low. Moreover, *X. birchmanni* and *X. variatus* are sympatric
424 over much of *X. birchmanni*'s range, but there has been no evidence of hybridization outside of
425 the three-way hybrids reported here (Kallman & Kazianis 2006).

426 The lack of evidence for contemporary hybridization involving *X. variatus*, *X.*
427 *birchmanni* or *X. birchmanni* x *X. malinche* hybrids outside of the Tlalica site and nearby sites
428 suggests that something is unique about this locality. We predict that the demography of the
429 Tlalica community and its disrupted water quality and chemistry play an important role in this
430 unusual hybridization event. Anthropogenic disturbance via wastewater effluent and landfill
431 leachate could have facilitated hybridization via two mechanisms: 1) by decreasing the
432 abundance of *X. birchmanni* x *X. malinche* hybrids with respect to *X. variatus* and 2) by
433 disrupting sensory cues used in mate choice.

434 *X. birchmanni*, *X. malinche*, and their hybrids are more sensitive to poor water quality
435 than *X. variatus* (Mercado-Silva *et al.*, 2006; personal observation), and *X. variatus* individuals
436 vastly outnumber *X. birchmanni* x *X. malinche* hybrids at the Tlalica site. Notably, nowhere else

437 on the Rio Calnali have we observed such a strong demographic skew toward *X. variatus*. Past
438 research has suggested that female mate preferences can weaken when the density of
439 conspecifics is low and encounter rate with heterospecifics is high, or the search cost of finding a
440 conspecific mate is very high (Cotton *et al.* 2006; Lehmann 2007; Verzijden *et al.* 2011; Stoffer
441 & Uetz 2015; Delclos *et al.* 2020), including in *X. birchmanni*, *X. malinche*, and *X. variatus*
442 (Fisher & Rosenthal, 2010). This raises the possibility that female *X. birchmanni* x *X. malinche*
443 hybrids mated with *X. variatus* males because there were so few Northern swordtail mates
444 available. This hypothesis is further supported by the lack of *X. variatus* mitochondrial ancestry
445 in three-way hybrids (Table S5). In *Xiphophorus*, females tend to have much stronger
446 conspecific mate preferences than males (Rosenthal & Garcia de Leon, 2011) and *X. variatus*
447 females in the Tlalica population have access to many conspecific males.

448 In addition to demography, our results are consistent with a role of anthropogenic shifts
449 in water quality and chemistry in this rare hybridization event. In many *Xiphophorus* species,
450 female mate choice is driven in large part by species-specific olfactory signals (Crapon De
451 Caprona and Ryan 1990; McLennan and Ryan, 1999; Wong *et al.* 2005; Fisher & Rosenthal
452 2006; Rosenthal *et al.* 2011; Verzijden *et al.* 2011). Research has shown that organic and
453 inorganic substances can alter the ability of female *X. birchmanni* to distinguish conspecific from
454 heterospecific males (Fisher, Wong, & Rosenthal, 2006, Powell *et al.* 2022). Levels of several
455 chemicals observed at Tlalica may be sufficient to disrupt olfactory communication and drive
456 hybridization between *X. variatus* and *X. birchmanni* x *X. malinche* hybrids. Elevated dissolved
457 organic matter has been shown to impair chemical and/or visual communication in some fish
458 species at concentrations of ~1 mg/L of humic acid (Hubbard *et al.*, 2002; Mobley *et al.*, 2020),
459 similar to concentrations found in Tlalica and Calnali (Table S6). Ammonia can impair
460 generation of electric impulses in neurons and lead to health effects at low concentrations (1.3-
461 3.5 mg N/L; Ip, Chew, and Randall 2001). Because ammonia was found at concentrations above
462 toxic thresholds at Tlalica (Fig. 2), future research should test hypotheses regarding whether
463 ammonia affects mating behavior. Finally, the copper concentrations detected at Tlalica were
464 similar to the concentrations reported to disturb olfactory perception and olfactory-mediated
465 behaviors in other fish species (~2 µg/L; Sandahl *et al.*, 2007; Morris *et al.*, 2019).

466 Although *Xiphophorus* respond most strongly to olfactory sexual signals, visual cues are
467 also important in mating decisions (Crapon de Caprona and Ryan, 1990; McLennan and Ryan,
468 1999; Fisher *et al.*, 2006b; Verzijden and Rosenthal 2011; Delclos *et al.* 2020). Thus, the
469 increased turbidity of water at Tlalica and nearby sites may also play a role in the breakdown of
470 reproductive barriers (Seehausen *et al.* 1997). Turbid waters could indirectly facilitate
471 hybridization among *X. variatus* and *X. birchmanni* x *X. malinche* by disturbing the transmission
472 of visual cues involved in species/mate recognition. Testing hypotheses about the impacts of
473 water chemistry on mate choice using both chemical treatments and mate choice trials is an
474 exciting avenue for future investigation (e.g. as in Fisher *et al.*, 2006).

475 What are the consequences of the complex hybridization events that researchers are
476 beginning to uncover? One possible outcome when three species hybridize is the potential for
477 gene flow between two species that would otherwise not contact each other. Such “conduit
478 introgression” has been described in several systems (Heliconius Genome Consortium 2012;
479 Toews *et al.* 2018; Langdon *et al.* 2019; Grant and Grant 2020, Natola *et al.* 2022). While the
480 scenario uncovered at Tlalica is more complex since hybridization is occurring between pure *X.*
481 *variatus* and *X. birchmanni* x *X. malinche* hybrids, the effects on dynamics of gene flow could be
482 similar. Specifically, because *X. malinche* does not overlap with *X. variatus*, admixture with *X.*

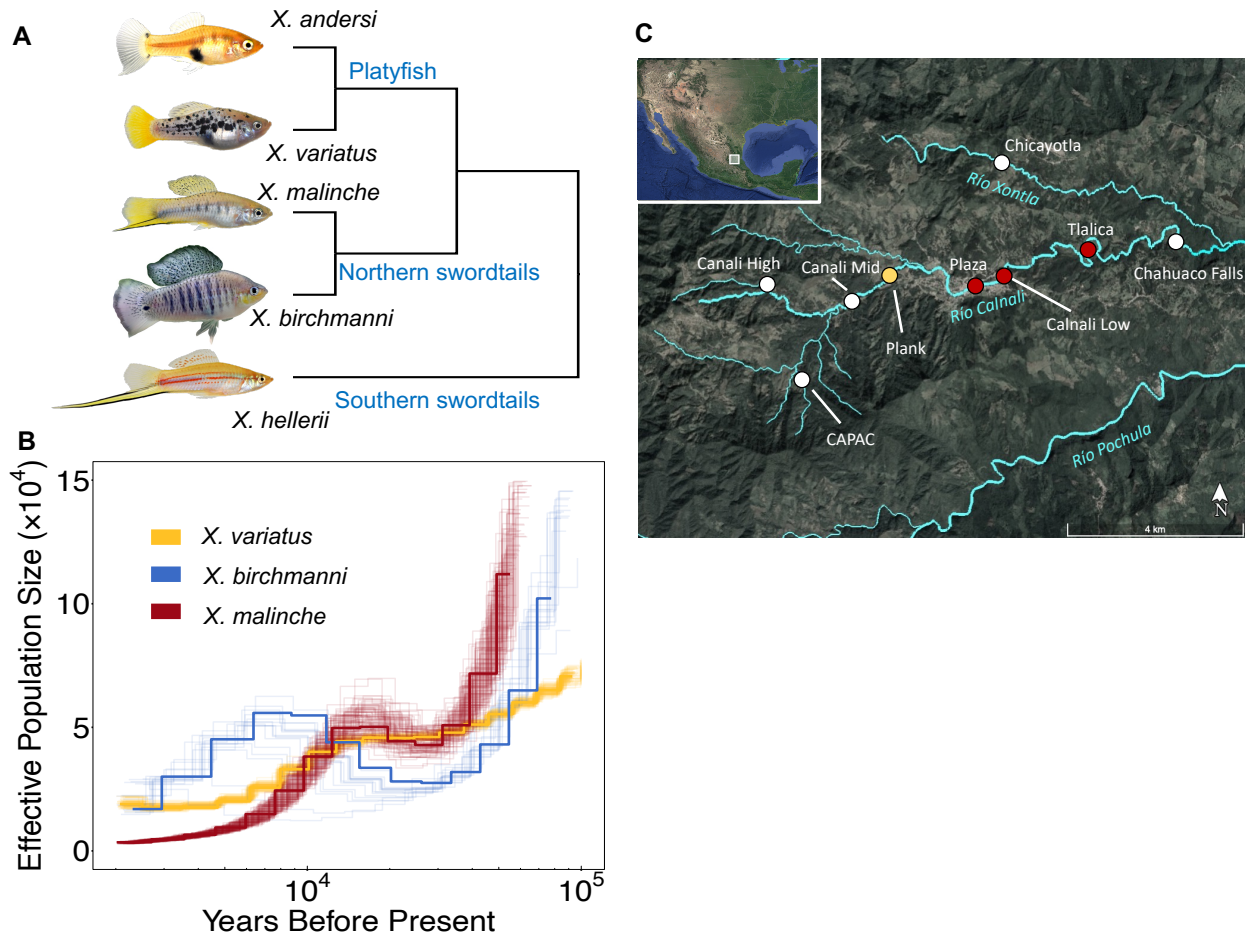
483 *birchmanni* x *X. malinche* hybrids could be a route for contemporary gene flow between *X.*
484 *variatus* and *X. malinche*.

485

486 *Conclusions*

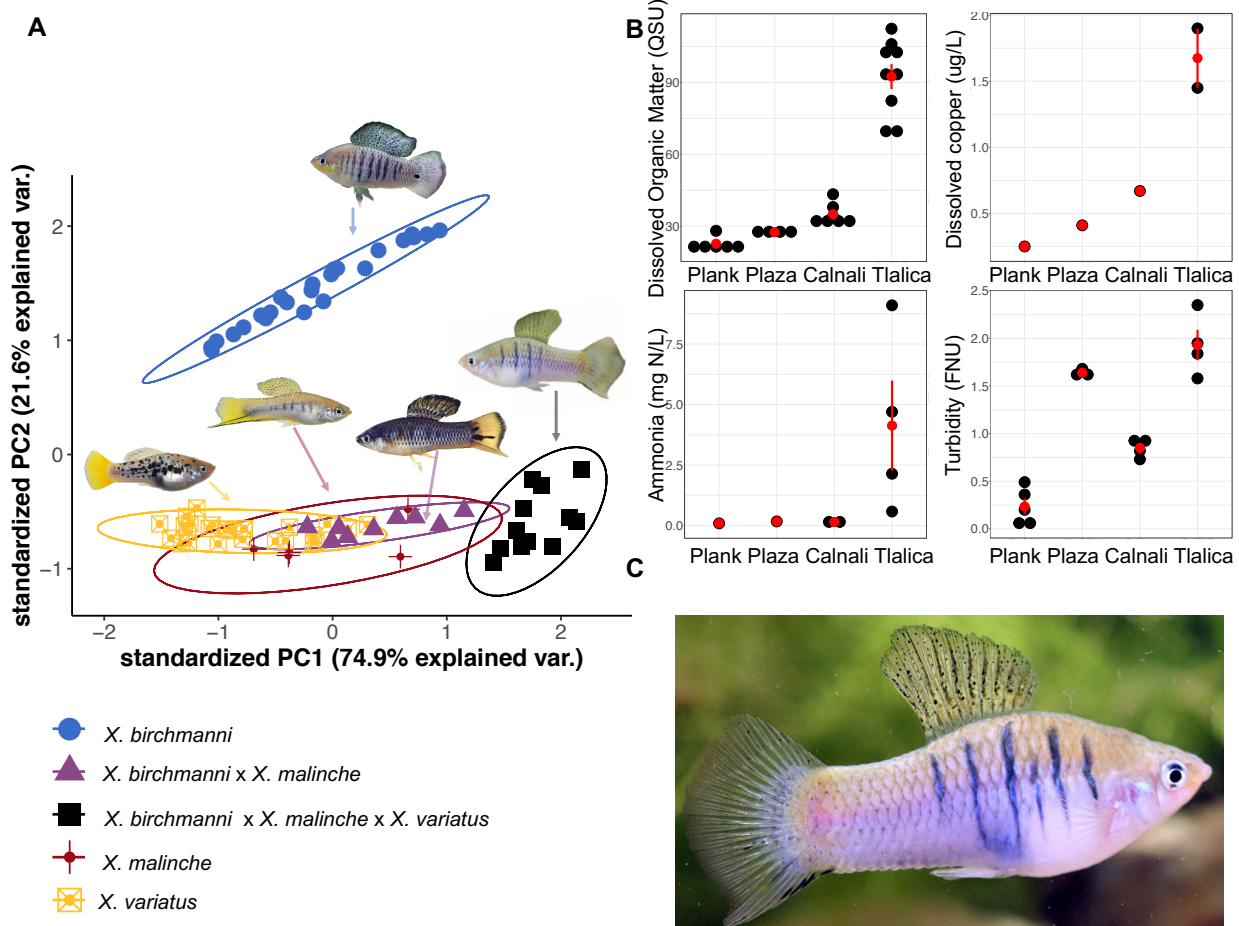
487 We present evidence of a deep hybridization event between the platyfish and Northern
488 swordtail clade, involving genetic material from three source species. Given the abundance of
489 first-generation three-way hybrids over multiple sampling seasons and the rarity of second
490 generation or later hybrids in our sample, we predict that there are significant costs in terms of
491 viability or fertility of this distant cross. While contemporary hybrids between these species have
492 not been previously reported, ancient hybridization between them has been inferred (Schumer *et*
493 *al.* 2018). Our data suggest that this unusual hybridization event may be linked to anthropogenic
494 disturbance in the local environment. Disentangling the mechanisms through which
495 anthropogenic disturbance contributes to hybridization in this system in an exciting direction for
496 future work.
497

498 **Figures**

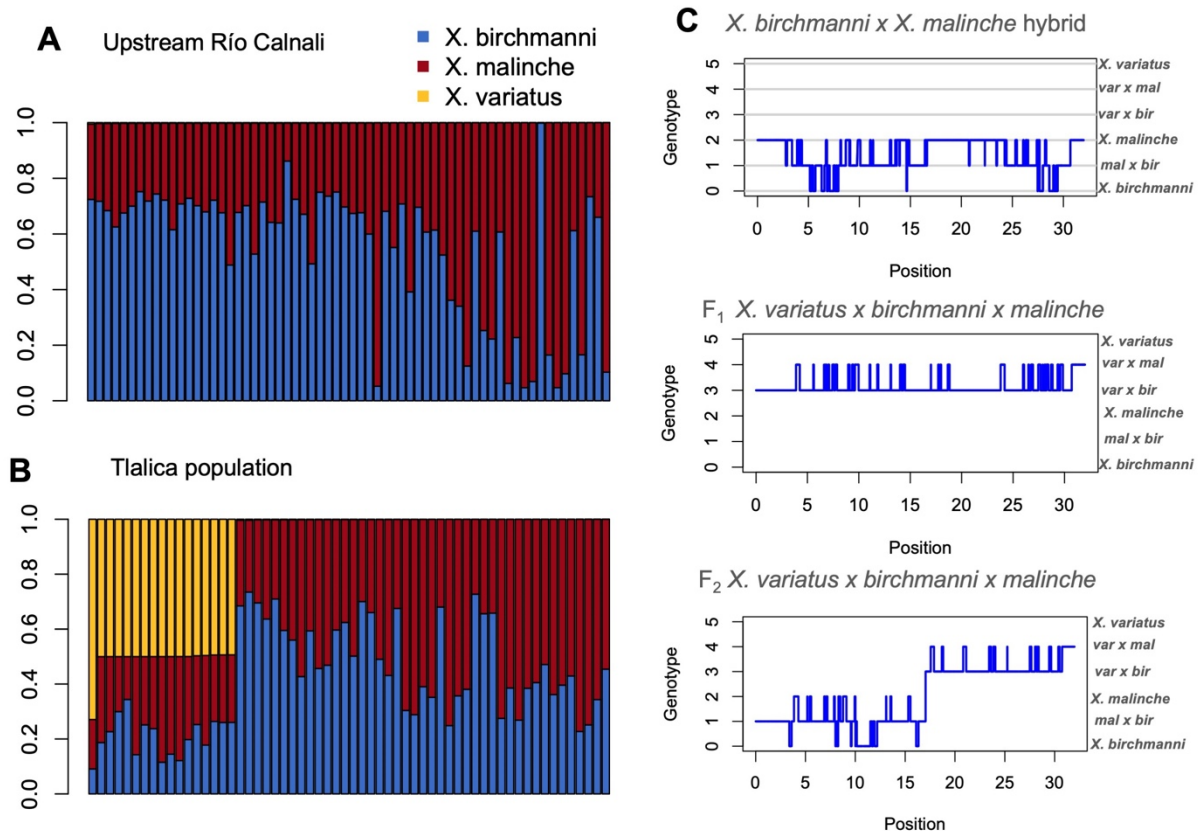


499
500 **Figure 1.** A) Simplified phylogeny of the genus *Xiphophorus*. *X. birchmanni* and *X. malinche*
501 are sister species in the Northern swordtail clade and *X. variatus* belongs to the distantly related
502 platyfish clade. B) PSMC results analyzing population history from a single whole-genome
503 sample of *X. variatus* and previously collected data from *X. birchmanni* and *X. malinche* (from
504 Schumer *et al.* 2018). Analysis was conducted with a ρ/θ ratio of 2, generation time of two
505 generations per year, and mutation rate of 3.5×10^{-9} . Faint lines reflect bootstrap resampling of
506 the data. C) Map of collection sites along the Río Calnali with the focal sites where three-way
507 hybrids have been collected highlighted in red, and upstream site used for comparison in water
508 quality and chemistry samples highlighted in yellow. Inset shows location of *X. birchmanni* x *X.*
509 *malinche* hybrid populations in Hidalgo, Mexico relative to a map of North and Central America.
510 Images adapted from Google Earth.

511
512



513
 514 **Figure 2. A)** Principal component analysis of morphology of male *X. malinche*, *X. birchmanni*,
 515 *X. variatus*, *X. birchmanni* x *X. malinche* hybrids and confirmed three-way hybrids. **B)** Dissolved
 516 organic matter (quinine sulfite units - QSU), ammonia (mg N/L), dissolved copper (ug/L), and
 517 turbidity (formazin nephelometric units - FNU) levels measured at Plank, Plaza, Calnali Low
 518 (Calnali), and Tlalica in May and June of 2022. Black dots represent independent measurements,
 519 red dots represent means, and red bars show one standard error of repeated measurements. **C)**
 520 Example of a first generation hybrid individual with 50% *X. variatus* ancestry, 23.8% *X.*
 521 *birchmanni* ancestry, and 26.2% *X. malinche* ancestry. This individual has a short sword, a trait
 522 which is unique to *X. malinche*, and large dorsal fin characteristic of *X. birchmanni*, and an
 523 overall body shape and vertical barring characteristics of *X. variatus*.
 524
 525



526
527 **Figure 3.** **A)** Distribution of genome-wide ancestry for individuals collected upstream of the
528 Tlalica site on the Río Calnali (N=553, downsampled for visualization to 64). Stacked plots
529 show the estimated proportion of each individual's genome derived from *X. variatus* (yellow), *X.*
530 *birchmanni* (blue), and *X. malinche* (red) based on local ancestry inference with *ancestryinfer*.
531 Individuals sampled from upstream sites have near-zero introgression from *X. variatus*. **B)**
532 Distribution of genome-wide ancestry for individuals with suspected swordtail ancestry collected
533 at the Tlalica site on the Río Calnali (N=64). Stacked plots show the estimated proportion of
534 each individual's genome derived from *X. variatus* (yellow), *X. birchmanni* (blue), and *X.*
535 *malinche* (red). While some *X. birchmanni* x *X. malinche* hybrid individuals sampled from
536 Tlalica lack *X. variatus* ancestry, a substantial proportion derive some of their genome from *X.*
537 *variatus*. **C)** Local ancestry inferred along chromosome 1 for individuals of different hybrid
538 types. The genotype on the y-axis corresponds to the ancestry class at that marker: 0 –
539 homozygous *X. birchmanni*, 1 – heterozygous *X. birchmanni* x *X. malinche*, 2 – homozygous *X.*
540 *malinche*, 3 – heterozygous *X. birchmanni* x *X. variatus*, 4 – heterozygous *X. malinche* x *X.*
541 *variatus*, 5 – homozygous *X. birchmanni*. In the top plot, a typical *X. birchmanni* x *X. malinche*
542 hybrid from the Río Calnali is shown. In the middle plot, a first generation hybrid between an *X.*
543 *birchmanni* x *X. malinche* mother and *X. variatus* father is shown (parental source populations
544 inferred based on mitochondrial ancestry, Table S5). Note that across the entire chromosome this
545 individual is either heterozygous *X. birchmanni* x *X. variatus* or heterozygous *X. malinche* x *X.*
546 *variatus* (genotype classes 3 or 4). In the bottom plot, ancestry for a “backcrossed” three-way

547 hybrid individual is shown. This individual is inferred to be the offspring of a first generation
548 three-way hybrid and a *X. birchmanni* x *X. malinche* mother. Note that this individual is
549 heterozygous for *X. variatus* ancestry over only approximately half of its chromosome.

550 **Acknowledgements**

551

552 We thank Heidi Fisher, Vitor Sousa, Gil Rosenthal, Claudia Bank, and members of the Schumer
553 and Rochman labs for helpful discussion and/or feedback on earlier versions of this work. We
554 are grateful to the Mexican federal government for permission to collect samples (Permiso de
555 Pesca de Fomento no. PPF/DGOPA-064/20). We thank Stanford University and the Stanford
556 Research Computing Center for providing computational support for this project. This work was
557 supported by NSF GRFP 2019273798 to B. Moran, NSF PRFB (2010950) to Q. Langdon, and a
558 Human Frontiers in Science Grant to M. Schumer & C. Rochman (RGY0081). The authors
559 declare no conflicts of interest.

560

561 **Author contributions**

562

563 S.M. Banerjee, D.L. Powell, and M. Schumer conceived of this project. S.M. Banerjee, D.L.
564 Powell, B.M. Moran, T. Gunn, and W.F. Ramírez-Duarte collected data, S.M. Banerjee, D.L.
565 Powell, B.M. Moran, Q. Langdon, W.F. Ramírez-Duarte, and M. Schumer analyzed data. M.
566 Schumer adapted *ancestryinfer* for three-way local ancestry inference. M. Schumer and C.
567 Rochman oversaw the project. All authors wrote the manuscript.

568

569 **Data availability**

570

571 All raw sequencing data for this project will be deposited on NCBI's SRA. All water quality and
572 chemistry data and ancestry calls will be deposited on Dryad. Computational pipelines and
573 analysis scripts are available at <https://github.com/Schumerlab>.

574

575

576

577

578

579

580

581

582

583

584

585

586

587

588

589

590

591

592

593

594

595

596

597 **References**

598

599 Armstrong, J., Hickey, G., et al. (2020). Progressive Cactus is a multiple-genome aligner for the
600 thousand-genome era. *Nature* 587, 246–251.

601 Borowsky, R. (1981). Tailspots of *Xiphophorus* and the evolution of conspicuous polymorphism.
602 *Evolution* 35(2), 345–358.

603 Chen, F. & Li, W. (2001). Genomic divergences between humans and other hominoids and the
604 effective population size of the common ancestor of humans and chimpanzees. *Am J Hum Genet*
605 68:2, 444-456.

606 Chunco, A. (2014). Hybridization in a warmer world. *Ecol Evol.* 2014 May;4(10):2019-31.

607 Corbett-Detig, R. & Nielsen, R. (2017). A Hidden Markov Model approach for simultaneously
608 estimating local ancestry and admixture time using next generation sequence data in samples of
609 arbitrary ploidy. *PLOS Genet*, 13, e1006529.

610 Cotton, S., Small, J., Pomiankowski, A. (2006). Selection and condition-dependent mate
611 preferences. *Curr Biol* 16:PR755-R765.

612 Crapon De Caprona, M. & Ryan, M. J. (1990). Conspecific mate recognition in swordtails,
613 *Xiphophorus nigrensis* and *X. pygmaeus* (Poeciliidae): olfactory and visual cues. *Anim*
614 *Behav* 39, 290-296.

615 Cui, R., Schumer, M., Kruesi, K., Walter, R., Andolfatto, P. & Rosenthal, G. (2013).

616 Phylogenomics reveals extensive reticulate evolution in *Xiphophorus* fishes. *Evolution*, 67,
617 2166–2179.

618 Culumber, Z. & Rosenthal, G. (2013). Mating preferences do not maintain the tailspot
619 polymorphism in the platyfish, *Xiphophorus variatus*, *Behav Ecol*, 24: 1286–1291.

620 Culumber, Z. (2014). Pigmentation in *Xiphophorus*: An emerging system in ecological and
621 evolutionary genetics. *Zebrafish* 11, 57–70.

622 Danecek P, Bonfield JK, et al. (2021). Twelve years of SAMtools and BCFtools. *Gigascience*
623 10(2):giab008

624 Delclos, P., Forero, S., Rosenthal, G. (2020). Divergent neurogenomic responses shape social
625 learning of both personality and mate preference. *J Exp Biol* 223(6): jeb220707.

626 Fisher, H. & Rosenthal, G. (2006) Female swordtail fish use chemical cues to select well-fed
627 mates. *Anim Behav* 72:721-725.

628 Fisher, H.S., Wong, B.B.M. & Rosenthal, G.G. (2006). Alteration of the chemical environment
629 disrupts communication in a freshwater fish. *Proc R Soc London Ser B*, 273, 1187–1193.

630 Fisher, H.S. & Rosenthal, G.G. (2010). Relative abundance of *Xiphophorus* fishes and its effect
631 on sexual communication. *Ethology*, 116: 32-38.

632 Grant, P. & Grant, R. (2020). Triad hybridization via a conduit species. *Proc Nat Acad Sci*
633 117(14): 7888-7896.

634 The Heliconius Genome Consortium. (2012). Butterfly genome reveals promiscuous exchange of
635 mimicry adaptations among species. *Nature* 487, 94–98.

636 Hubbard, P.C., Barata, E.N., Canario, A.V.M. (2002). Possible disruption of pheromonal
637 communication by humic acid in the goldfish, *Carassius auratus*. *Aquat Toxicol* 60, 169–183.

638 Ip, Y.K., Chew, S.F., Randall, D.J (2001). Ammonia toxicity, tolerance, and excretion.
639 *Fish Physiol* 20: 109–148.

640 Kallman, K. & Kazianis, S. (2006). The genus *Xiphophorus* in Mexico and Central America.
641 *Zebrafish*. 3:271-285.

- 642 Kelly, B., Whiteley, A., Tallmon, D. (2010). The Arctic melting pot. *Nature* 468, 891.
- 643 Langdon, Q.K., Peris, D., Kyle, B., Hittinger, C.T. (2018). sppIDer: a species identification tool
644 to investigate hybrid genomes with high-throughput sequencing. *Mol Biol Evol*, 35, 2835–2849.
- 645 Langdon, Q.K., Peris, D., et al. (2019). Fermentation innovation through complex hybridization
646 of wild and domesticated yeasts. *Nat Ecol Evol* 3, 1576–1586.
- 647 Lehmann (2006). Density-dependent plasticity of sequential mate choice in a bushcricket
648 (Orthoptera : Tettigoniidae). *Austral J Zool* 55(2): 123-130.
- 649 Li, H. & Durbin, R. (2009). Fast and accurate short read alignment with Burrows-Wheeler
650 Transform. *Bioinformatics*, 25:1754-60.
- 651 Li, H., & Durbin, R. (2011). Inference of human population history from individual whole-
652 genome sequences. *Nature* 475, 493–496.
- 653 McLennan, D. A. & Ryan, M. J. (1999). Interspecific recognition and discrimination based upon
654 olfactory cues in northern swordtails. *Evolution* 53, 880-888.
- 655 Mercado-Silva, N., Lyons, J., et al. (2006). Long-term changes in the fish assemblage of the Laja
656 River, Guanajuato, central Mexico. *Aquatic Conserv: Mar. Freshw. Ecosyst.*, 16: 533-546.
- 657 Mobley, R.B., Weigel, E.G., Boughman, J.W. (2020). Does humic acid alter visually and
658 chemically guided foraging in stickleback fish? *Anim Cogn* 23, 101–108.
- 659 Moran, B.M., Payne, C.Y., et al. (2021). A lethal genetic incompatibility between naturally
660 hybridizing species in mitochondrial complex I. bioRxiv. doi:
661 <https://doi.org/10.1101/2021.07.13.452279>
- 662 Moran, B.M., Payne, C., Langdon, Q., Powell, D.L., Brandvain, Y., Schumer, M. (2021). The
663 genomic consequences of hybridization. *eLife*, 10, e69016.
- 664 Morris, J.M., Brinkman, S.F., Takeshita, R., McFadden, A.K., Carney, M.W., Lipton, J. (2019).
665 Copper toxicity in Bristol Bay headwaters: part 2—olfactory inhibition in low-hardness water.
666 *Environ Toxicol Chem* 38, 198–209.
- 667 Natola, L., Seneviratne, S. S., Irwin, D. (2022). Population genomics of an emergent tri-species
668 hybrid zone. *Mol Ecol* 00, 1– 12.
- 669 Ottenburghs, J. (2020). Ghost introgression: spooky gene flow in the distant past. *BioEssays*, 42,
670 2000012.
- 671 Oziolor, E.M., Reid, N.M., et al. (2019). Adaptive introgression enables evolutionary rescue
672 from extreme environmental pollution. *Science*, 364, 455–457.
- 673 Pampoulie, C., Gíslason, D., et al. (2021). Evidence of unidirectional hybridization and second-
674 generation adult hybrid between the two largest animals on Earth, the fin and blue whales. *Evol*
675 *Appl* 14: 314– 321.
- 676 Payne, C., Bovio, R., et al. (2022). Genomic insights into variation in thermotolerance between
677 hybridizing swordtail fishes. *Mol Ecol*.
- 678 Powell, D.L., García-Olazábal, et al. (2020). Natural hybridization reveals incompatible alleles
679 that cause melanoma in swordtail fish. *Science*, 368, 731–736.
- 680 Powell, D.L., Moran, B.M., et al. (2021). Two new hybrid populations expand the swordtail
681 hybridization model system. *Evolution*, 75, 2524–2539.
- 682 Rauchenberger, M., Kallman, K.D., Morizot, D.C. (1990). Monophyly and geography of the Río
683 Pánuco Basin swordtails (genus *Xiphophorus*) with descriptions of four new species. *Am Mus*
684 *Nov no.* 2975.
- 685 Rosenthal, G.G., Rosa Reyna, X.F., et al. (2003). Dissolution of sexual signal complexes in a
686 hybrid zone between the swordtails *Xiphophorus birchmanni* and *Xiphophorus malinche*
687 (Poeciliidae). *Copeia* 299–307.

- 688 Rosenthal, G.G. & Garcia de Leon, F.J. (2011). Speciation and hybridization. In: (*Ecology and*
689 *evolution of poeciliid fishes*), 109–119.
- 690 Rosenthal, G., Fitzsimmons, J.N., Woods, K.U., Gerlach, G., Fisher, H.S. (2011). Tactical
691 release of a sexually-selected pheromone in a swordtail fish. PLoS ONE 6(2): e16994.
- 692 Sandahl, J.F., Baldwin, D.H., Jenkins, J.J., Scholz, N.L. (2007). A sensory system at the interface
693 between urban stormwater runoff and salmon survival. Environ Sci Technol 41,
694 2998–3004.
- 695 Schneider, C. A., Rasband, W. S., Eliceiri, K. W. (2012). NIH Image to ImageJ: 25 years of
696 Image Analysis. Nat Methods, 9(7), 671–675.
- 697 Schumer, M., Cui, R., Powell, D.L., Dresner, R., Rosenthal, G.G., Andolfatto, P. (2014). High-
698 resolution mapping reveals hundreds of genetic incompatibilities in hybridizing fish species.
699 eLife, 3, e02535.
- 700 Schumer, M., Powell, D.L., et al. (2017). Assortative mating and persistent reproductive
701 isolation in hybrids. Proc Nat Acad Sci, 114, 10936.
- 702 Schumer, M., Xu, C., et al. (2018). Natural selection interacts with recombination to shape the
703 evolution of hybrid genomes. Science, 360, 656.
- 704 Schumer, M., Powell, D.L., Corbett-Detig, R. (2020). Versatile simulations of admixture and
705 accurate local ancestry inference with mixnmatch and ancestryinfer. Mol Ecol Res, 20, 1141–
706 1151.
- 707 Seehausen, O., Alphen, J., Witte, F. (1997). Cichlid fish diversity threatened by eutrophication
708 that curbs sexual selection. Science, 277, 1808–1811.
- 709 Stoffer, B., Uetz, G.W. (2015). The effects of social experience with varying male availability on
710 female mate preferences in a wolf spider. Behav Ecol Sociobiol 69, 927–937.
- 711 Toews, D., Streby, H., Burket, L., Taylor, S. (2018). A wood-warbler produced through both
712 interspecific and intergeneric hybridization. Biol Lett.
- 713 Vallejo-Marín, M. Hiscock, S.J. (2016). Hybridization and hybrid speciation under global
714 change. New Phytol, 211: 1170-1187.
- 715 Van der Auwera, G.A. & O'Connor, B.D. (2020). Genomics in the cloud: Using Docker, GATK,
716 and WDL in Terra (1st Edition). O'Reilly Media.
- 717 Verzijden, M. & Rosenthal, G. (2011). Effects of sensory modality on learned mate preferences
718 in female swordtails. Anim Behav 82(3): 557-562.
- 719 Willis, P.M., Ryan, M.J., Rosenthal, G.G. (2011). Encounter rates with conspecific males
720 influence female mate choice in a naturally hybridizing fish. Behav Ecol, 22, 1234–1240.
- 721 Wong, B., Fisher, H., Rosenthal, G. (2005). Species recognition by male swordtails via chemical
722 cues. Behav Ecol 16(4): 818–822
- 723 Wu, J., Liu, Y., Zhao, Y. (2021). Systematic review on local ancestor inference from a
724 mathematical and algorithmic perspective. Front Genet.